Selective pressures on C_4 photosynthesis evolution in grasses through the lens of optimality

Haoran Zhou[1], Brent R. Helliker[1] and Erol Akçay[1]

[1] Department of Biology, University of Pennsylvania, Philadelphia, PA 19104, USA

Correspondence: Haoran Zhou

Phone: 1-215-808-7042

Email: haoranzh@sas.upenn.edu

Brent R. Helliker*: helliker@sas.upenn.edu*

Erol Akçay: *eakcay@sas.upenn.edu*

Statement of authorship: HZ, BH and EA came up with the idea. HZ and EA built the model, BH put the idea in a general historical context, HZ performed the modeling work and analyzed output data. HZ wrote the first draft, BH and EA contributed substantially to revisions.

Keywords cost of C_4, evolution, optimal stomatal conductance, root-leaf allocation, water limitation, CO_2, temperature, light intensity, nitrogen allocation, dark/light reaction

Conflict of interest: None declared.

Abstract

CO_2, temperature, water availability and light intensity were potential selective pressures to propel the initial evolution and global expansion of C_4 photosynthesis in grasses. To tease apart the primary selective pressures along the evolutionary trajectory, we coupled photosynthesis and hydraulics models and optimized photosynthesis over stomatal resistance and leaf/fine-root allocation. We also examined the importance of nitrogen reallocation from the dark to the light reactions. Our results show that the higher stomatal resistance and leaf/root allocation ratio conferred by the C_4 photosynthesis led to C_4 advantage without any change in hydraulic conductance. For the initial evolution of C_4 25-32 MYA, water limitation was the primary driver, and N reallocation was necessary. Low CO_2, together with light intensity, were the primary drivers during the global radiation of C_4 5-10 MYA, during this period N reallocation would not have been strongly selected.

Introduction

Understanding the evolution of C_4 photosynthesis and the global distribution of C_3 and C_4 grasses are central questions in macro-level plant evolution and ecology. Costs and benefits of the carbon concentrating mechanism (CCM) of C_4 grasses in different climates are key to deal with these questions. Physiological models of photosynthesis focused on examining temperature and CO_2 concentration as selective pressures for C_4 evolution and expansion (Ehleringer & Monson 1993, Ehleringer et al. 1997, Collatz et al.

1998). They demonstrate that under warmer temperatures and low CO_2 concentration, the CCM leads to less photorespiration and hence greater carbon gain in C_4, but in cooler and high CO_2, the metabolic costs of the CCM and lower photorespiration leads to greater carbon gain in C_3. In evolutionary terms, it is thought that as grasslands expanded through the late Oligocene and early Miocene (Osborne 2008, Strömberg 2011), the concomitant drop in CO_2 concentration and subsequent carbon starvation leading to an increase in photorespiration and the impetus for C_4 evolution in the grasses. A further drop in CO_2 concentration in the late Miocene was hypothesized to have led to the global-scale radiation of C_4 5-10 MYA (Edwards et al. 2010, Sage et al. 2012).

Recent phylogenetic evidence has, however, challenged the traditional thinking about the controls on current distribution and the evolutionary impetus for C_4 in the grasses. Notably, the PACMAD clade, which contains all C_4 grasses, is distributed in warm areas regardless of photosynthetic pathway, whereas the BEP clade containing no C_4 grasses predominates in cold areas (Edwards & Still 2008). Thus, the current global distribution of C_3 and C_4 grasses might be a consequence of traits inherited from separate evolutionary lineages, as opposed to differential temperature responses between C_3 and C_4 photosynthesis. Additionally, water availability has emerged as a potential primary selective agent in the evolution of C_4 (Edwards & Still 2008, Edwards & Smith 2010), and a major contributor to current distribution of C_3 and C_4 species within a clade (Pau et al.

2013). C_4 photosynthesis is thought to have a higher water-use-efficiency (WUE) than C_3 because the CCM allows for C_4 to maintain a lower stomatal conductance for a given assimilation rate (Ghannoum 2009, Taylor et al. 2014). Enhanced WUE has long been suspected as the impetus for the evolution of C_4 in dicotoledenous plants (Sage 2004, Edwards & Smith 2010). The potential role of water limitation in C_4 grass evolution has sparked increased interest in explaining both current distributions and the anatomical shifts in C_3 grasses that were prerequisites to C_4 evolution (Griffiths et al. 2012, Osborne & Sack 2012, Taylor et al. 2012).

It is also likely that different selection pressures contributed to the initial evolution and subsequent spread of C_4 photosynthesis. Estimates of CO_2 concentrations during the initial period of C_4 evolution in the grasses 25-32 MYA, range between 350-550 ppm (Cerling et al. 1997, Kürschner et al. 2008, Edwards et al. 2010, Sage et al. 2012). At the low end of this range, there would likely be selection for the evolution of C_4 via the carbon-starvation hypothesis, but not at the high end. On the other hand, there is a general consensus that low CO_2 led to the expansion of C_4 grasses from 5-10 MYA, but recent phylogenetically-based analyses show that other factors, especially water availability, may play more important roles in the radiation of C_4 grasses and expansion of C_4 grassland (Edwards & Smith 2010, Osborne & Freckleton 2009, Griffiths et al. 2012, Osborne & Sack 2012).

A related but largely unstudied evolutionary change during the divergence of C_4 photosynthesis from C_3 is the allocation of nutrients between the dark reactions and the light reactions. C_4 plants might allocate a greater proportion of N to light reactions than to dark reactions as compared to C_3 because of the extra ATP costs of the CCM (Tissue et al. 1995, Ghannoum et al 2010). We propose that the reallocation of N between dark and light reactions provides a further advantage for C_4 above the CCM alone, and that different environmental conditions can select for a shift in the degree of reallocation both through evolutionary time and across species in extant plants.

The physiology and phylogeographic patterns of C_4 thus suggest multiple environmental drivers might have interacted to select for C_4 evolution. Our goal in this paper is to tease apart the selective pressures that led to the evolution of C_4 photosynthesis initially, its global expansion 5-10 MYA, and its current distribution within the framework of an optimality model in which the plant makes allocation “decisions” in order to maximize its photosynthetic assimilation rate. To do this, we revisit the temperature-CO_2 crossover approach and integrate the effects of water limitation, light, optimal allocation decisions, and the interactions between these in a single model. Specifically, our model advances our understanding of C_4 evolution in four important ways. First, few modeling studies have explicitly considered multiple factors and their interactions. We incorporate water availability and light intensity as selective factors in addition to temperature and CO_2. Second, the hypothesis that C_4 photosynthesis has a higher WUE than C_3 implicitly relies on an optimality argument to balance carbon gain and water loss (Medlyn et al. 2011, Prentice et al. 2014), yet the role of optimal stomatal conductance in mediating selective pressures due to water limitation during the evolution of C_4 plants remains largely unexplored (but see Way et al. 2014). Most previous models assume *a priori* that C_4 grasses have lower stomatal conductance. Instead, we let both stomatal resistance and leaf/fine-root allocation emerge endogenously from the model using optimality arguments. Third, we include the cost of the C_4 pathway in the light reactions (2 additional ATP per CO_2 fixed; Hatch 1987, von Caemmerer 2000), which previous models did not explicitly consider (Chen et al. 1994, Ehleringer et al. 1997, Collatz et al. 1992, Osborne & Sack 2012). Finally, we consider reallocation of nitrogen from the dark reactions to the light reactions, which can change the tradeoffs between photosynthesis and water use by C_4 grasses.

Model construction

Overview of the model

Different modeling scenarios are used to examine the advantage of C_4 during the initial origin, expansion and current distribution of C_4 photosynthesis. Initially, we assume that the CCM is the only difference between C_3 and C_4. This comparison corresponds to two closely related species whose other traits have not had time to diverge in response to differential selection pressures. Next, we examine shifts in N allocation between light and dark reactions of C_4, which may have happened in further divergence of C_3 and C_4 after the CCM evolved.

The soil-plant-air water continuum was incorporated in C_3 photosynthesis models (Farquhar et al. 1980) and C_4 models (von Caemmerer 2000) to examine interactions of CO_2, water availability, light and temperature. We used the optimality approach of Givnish (1986), where C_3 and C_4 plants optimize stomatal resistance and leaf/fine-root allocation to balance carbon gain and water loss. A full model description is in Supplementary Material I. The model derivation using Mathematica (Wolfram Research, Inc.) and methods for numerical solutions are in Supplementary Material II.

C_3 photosynthesis model

Considering the steady state of CO_2 diffusion in mesophyll cells, we get:

$$A_n = \frac{C_a - C_m}{r_s + r_m} \quad , \qquad (1)$$

where A_n is the net assimilation rate, C_a and C_m are the atmospheric and mesophyll CO_2 mixing ratios, and r_s and r_m is the stomatal and mesophyll resistance (the inverse of stomatal or mesophyll conductance). A_n is computed using the FvCB model (Farquhar et al. 1980) and is the minimum of two limitation states (eq. (4)): the Rubisco carboxylation (dark reaction) limitation state (A_c) (eq. (2)), low CO_2 and high light intensity cause a saturating supply of substrate (RuBP) for Rubisco, and reaction rate is controlled by the enzyme kinetics of Rubisco; the RuBP regeneration (light reaction) limitation state(A_j)

(eq. (3)), when light intensity is low and RuBP availability limits the reaction rate. The assimilation rates are given by:

$$A_c = \frac{V_{cmax,\psi_l}(C_m - \Gamma^*)}{C_m + K_c(1 + \frac{O_m}{K_o})} - R_d \qquad (2)$$

$$A_j = \frac{J_{max,\psi_l}(C_m - \Gamma^*)}{4.5C_m + 10.5\Gamma^*} - R_d \qquad (3)$$

$$A_n = min(A_c, A_j), \qquad (4)$$

where $V_{cmax,\psi l}$ is maximum velocity of Rubisco carboxylation (the subscript Ψ_l denotes it's a function of leaf water potential), $J_{max,\psi l}$ is maximum rate of electron transport at a specific light intensity, R_d is the mitochondrial respiration rate in the daytime and Γ^* is CO_2 compensation point of photosynthesis. O_m is O_2 concentration in the mesophyll cell, which is assumed equal to atmospheric O_2. K_c and K_o are the Michaelis-Menten constants of Rubisco for CO_2 and O_2.

C_4 photosynthesis model

For the C_4 pathway, we consider the steady state mixing ratio of CO_2 in both mesophyll (C_m) and bundle sheath cells (C_{bs}), which gives us two equations:

$$A_n = V_p - g_{bs}(C_{bs} - C_m) \qquad (5)$$

$$A_n = \frac{(C_a - C_m)}{(r_s + r_m)} + R_{dm}, \qquad (6)$$

where g_{bs} is the bundle sheath conductance, V_p is the PEP carboxylation rate, ($g_{bs}(C_{bs}-C_m)$) represents bundle sheath leakage from bundle sheath cells back to mesophyll and R_{dm} are the daytime mitochondrial respiration rate in mesophyll cells.

The PEP carboxylation rate V_p is limited by either PEPc carboxylation (eq. (7)), which follows a Michaelis-Menten type or PEP regeneration (eq. (8))

$$V_p = \frac{V_{pmax,\psi_l} C_m}{C_m + K_p} \quad (7)$$

$$V_p = x J_{max}/3 \quad , \quad (8)$$

where V_{pmax,ψ_l} is maximal PEPc carboxylation rate, K_p is the Michaelis-Menten coefficient of PEPc for CO_2 and x is the fraction of total electron transport could be used for the PEP regeneration, which represents the cost of the CCM. The denominator 3 in eq. (8) arises due to the fact that regeneration of 1 molecule of PEP needs 2 additional ATP, which is 3 additional electrons transported. Thus, equations (8) and (10) incorporate the cost of C_4 pathway. A_c and A_j of C_4 are given by

$$A_c = \frac{V_{cmax,\psi_l}(C_{bs} - \Gamma^*)}{C_{bs} + K_c(1 + \frac{O_{bs}}{K_o})} - R_d \quad (9)$$

$$A_j = \frac{(1-x) J_{max,\psi_l}(C_{bs} - \Gamma^*)}{4.5 C_{bs} + 10.5\Gamma^*} - R_d \quad (10)$$

which is obtained by substituting C_m in eq. (2) and (3) with C_{bs}.

Based on equations (7), (8), (9) and (10), A_n of C_4 is limited by four states as follows:

$$A_n = min(A_{cc}, A_{cj}, A_{jc}, A_{jj}) \quad . \quad (11)$$

Here, A_{cc} is RuBP carboxylation and PEPc carboxylation limited rate; A_{cj} is RuBP carboxylation and PEP regeneration limited rate; A_{cj} is PEP carboxylation and RuBP regeneration limited rate; and A_{jj} is limited by PEP regeneration and RuBP regeneration limited rate.

Hydraulic system

Eq. (12) describes the soil-plant-air continuum (Givnish 1986). At equilibrium, the rate of water loss through transpiration equals the rate of water absorption by the roots:

$$\frac{EfN}{\rho} = k(1-f)N(\psi_l - \psi_s) \quad , \qquad (12)$$

where Ψ_s is soil water potential, k is the effective root hydraulic conductivity, N is the total biomass of fine root and leaves, ρ is the leaf mass density (gcm^{-2}) and E is the transpiration rate per leaf area. E could be written as δ/r_s, where δ is the water partial pressure deficit between saturated leaf surface and the atmosphere. Thus, leaf water potential (Ψ_l) is a function of r_s and leaf/fine-root allocation (f, defined as investment into leaves/total investment in leaves and fine root)).

$$\psi_l = \psi_s - \frac{f\delta}{\rho k r_s(1-f)} \qquad (13)$$

Inhibition of photosynthesis by water stress

Reduced leaf water potential inhibits photosynthesis (Tezara et al. 1999, Lawlor & Cornic 2002, Tang 2002). We model this cost of transpiration as Weibull-type vulnerability curves relating leaf Ψ_l and photosynthetic parameters (Vico & Porporato 2008):

$$V_{cmax,\psi_l} = V_{cmax} e^{-(\frac{-\psi_l}{d_v})^{b_v}} \qquad (14)$$

$$J_{max,\psi_l} = J_{max} e^{-(\frac{-\psi_l}{d_j})^{b_j}} \qquad (15)$$

$$V_{pmax,\psi_l} = V_{pmax} e^{-(\frac{-\psi_l}{d_p})^{b_p}} \quad , \qquad (16)$$

where b and d are curve fitting parameters. Since Ψ_l is a function of r_s and f, all those parameters are functions of r_s and f.

Optimal stomatal resistance and optimal allocation of energy between leaves and fine roots

We assume that the plant adjusts the r_s and f to optimize the total carbon gain by

$$A_{total} = fNA_n/\rho \quad , \qquad (16)$$

where ρ is the leaf mass density (g cm^{-2}). As a simplifying assumption, we assume N and ρ are fixed (similar to Givnish, 1986). Effectively, we consider the optimization problem faced by the plant in a given instance during its growth, where its size (of which N is a proxy) can be regarded as a constant. Clearly, during plant growth, the assimilate will be turned into plant biomass, but the instantaneous optimization problem will still yield the optimal growth path, as it maximized the growth rate at any given time. Finally, we regard ρ as a species-specific trait that changes at a slower time-scale than r_s and f. The first order optimality conditions for r_s and f are given by (Givnish 1986):

$$\frac{\partial(fA_n)}{\partial r_s} = f\frac{\partial A_n}{\partial r_s} = 0 \qquad (17)$$

$$\frac{\partial(fA_n)}{\partial f} = A_n + f\frac{\partial(A_n)}{\partial f} = 0 \quad . \qquad (18)$$

We checked the second order derivative to ensure that the numerical solutions to the first order conditions were maxima.

Allocation of nitrogen

We examine how nitrogen allocation between RuBP carboxylation and RuBP regeneration in C_4 grasses affect competitive advantage over C_3 grasses. Despite great variation in V_{cmax} and J_{max} based on the total leaf nitrogen content within C_3 plants, Wullschleger (1993) found a mean of J_{max}/V_{cmax} =2.1 across 109 C_3 species, which we use as a baseline for C_3 and C_4 pathways in analyzing the initial evolution of C_4. Then, we used J_{max}/V_{cmax} =4.5 for C_4 (Vico & Porporato 2008, Osborne & Sack 2012) to analyze the role that nitrogen reallocation played in the evolutionary trajectory of C_4 plants. In determining the values of J_{max} and V_{cmax}, we used a simplified stoichiometry: we consider the total of J_{max} and V_{cmax} as a constant to hold nitrogen concentration constant (Vico & Porporato 2008, Osborne & Sack 2012). Two assumptions are underlying this simplified stoichiometry: (1) investing one molecule of nitrogen to the dark reactions will increase of V_{cmax} equal to the increase of J_{max} by investing one molecule of nitrogen to the light reactions; (2) nitrogen allocation to photorespiration and to the CCM balanced each other.

Modeling scenarios

We modeled the photosynthesis rates of C_3 and C_4 under temperature range from 10 °C to 40 °C with an interval of 5 °C, under CO_2 mixing ratios ranging from 200 ppm to 600 ppm with an interval of 50 ppm, under different water conditions (VPD=0.001, 1, 2, 3, 4kPa corresponding to soil water potential (Ψ_S) =0, -0.5, -1, -1.5, -2 MPa) and under different light intensities (1400, 1000, 600, 200, 100 µmol photons $m^{-2}s^{-1}$). We consider

VPD=0.001 kPa and Ψ_S =0 MPa as saturated water condition and light intensity of 1400 μmol photons $m^{-2} s^{-1}$ as an average saturated light intensity of a day.

Results

C_3/C_4 crossover temperatures and environmental variations

We numerically solved for assimilation-based crossover temperatures, defined as the temperature at which assimilation by the C_4 pathway starts exceeding that by the C_3, across the full range of CO_2, evaporative conditions, and soil-water availability, all under saturated light. In the first scenario (Fig. 1a), we assume the same allocation of N to light and dark reactions in the C_3 and C_4 plants (specifically, J_{max}/V_{cmax}=2.1 for both). Across all CO_2 concentrations, the crossover temperature decreases as water limitation increased. Under the most extreme water-stressed conditions (VPD = 4 kPa, Ψ_S =-2 MPa), the crossover temperatures are all below 5°C, even under a CO_2 of 600 ppm, and C_4 plants have an advantage at all temperatures.

In our second scenario, we assume a reallocation between RuBP regeneration and RuBP carboxylation processes in C_4 by changing the J_{max}/V_{cmax} ratio to 4.5 while keeping it at 2.1 in C_3 (Fig. 1b). The crossover temperatures are lower than the first scenario under saturated water conditions through to VPD = 3 kPa and Ψ_S = -1.5 MPa, suggesting that reallocation increases the advantage of C_4 in those conditions. Under low CO_2 and low water availability (e.g. CO_2=300 ppm, VPD = 3 kPa and Ψ_S = -1.5 MPa or all CO_2

concentrations with VPD = 4 kPa and Ψ_S = -2 MPa), however, crossover temperatures are comparatively higher than those of J_{max}/V_{cmax}=2.1, showing that reallocation decreases the C_4 advantage under water limitation and low CO_2.

Under saturated soil water availability, low VPD, and identical light- and dark-reaction allocation of C_3 and C_4, crossover temperatures decrease along with increasing light intensity (Fig. 1c). An increase in light intensity provides a larger relative benefit for C_4 at low CO_2, because C_3 photosynthesis is CO_2 limited and C_4 is light limited. The crossover temperatures under all light intensities reach 40 ^oC, when CO_2 is above 350 ppm. With the change of J_{max}/V_{cmax} (Fig. 1d), crossover temperatures decrease at every light intensity. The high-light result in Fig. 1d predicts a C_3/C_4 crossover temperature of 23°C under 380 ppm, similar to previous models that did not explicitly account for water stress (Ehleringer et al. 1997, Collatz et al 1998).

Stomatal resistance and leaf root allocation

Under all scenarios and both for C_3 and C_4 plants, optimal r_s first decreases as temperature increases, and then increases and it increases monotonically with increasing CO_2 (Fig. 2 a, c, e). Throughout the range of water availability we considered, optimal r_s is higher for C_4 than C_3 at temperature ranging from 10 to 40 ^oC and CO_2 ranging from 200 to 600 ppm. The optimal *f* has a similar relationship of an inverse U-shape curve along with temperature. Increasing CO_2 results in an increase of leaf allocation (Fig. 2 b, d, f). Optimal *f* for C_3 is always higher than that for C_4 under different water availability and CO_2. *f* decreases as intensity of water limitation increase. Results are the same for C_4 with a J_{max}/V_{cmax} of 4.5 (not shown).

RuBP carboxylation versus regeneration limitations

The C_3 pathway transitions from being CO_2 limited under low temperatures to light limited under high temperatures. The jumps in r_s and *f* in Fig. 2 correspond to the transition from RuBP carboxylation limited assimilation (A_c) to RuBP regeneration limited assimilation (A_j) of C_3, and the transition from RuBP carboxylation and PEP regeneration limited (A_{jc}) to RuBP regeneration and PEP regeneration limited assimilation (A_{jj}) of C_4. The transition temperature decreases as CO_2 increases. In the Fig. S1, A_c, A_j, A_{cc}, A_{cj}, A_{jc} and A_{jj} are plotted together under several environmental scenarios, using both J_{max}/V_{cmax}=2.1 and 4.5 for C_4. With J_{max}/V_{cmax}=2.1, C_4 is light limited in all the environmental conditions. With J_{max}/V_{cmax}=4.5, C_4 starts to be limited by CO_2 under low temperatures and to be limited by light under high temperatures.

Quantifying differences in C-assimilation rate

While crossover temperatures allow for a clear diagnostic of comparative assimilation, they do not demonstrate the degree of difference. To this end, we calculated the net assimilation rate difference between C_4 and C_3, ΔA_n (net assimilation of C_4 minus that of C_3), under different conditions (Fig. 3 and 4). Under a CO_2 concentration of 200 ppm and saturated light, ΔA_n is higher under moister conditions than water-limited conditions (Fig. 3a). In contrast, under higher CO_2 concentrations (400 and 600 ppm), C_4 has an advantage only in serious water limited conditions, which leave a relatively small scope for C_4 to evolve (areas where ΔA_n>0 in Fig. 3c, e). This result is due to the fact that C_3 photosynthesis has a greater proportional increase in assimilation from 200 to 400 and 600 ppm CO_2. However, the change of J_{max}/V_{cmax} increases both the ΔA_n and space for C_4 advantage (Fig. 3 b, d, f). Similar with water availability, at 200 ppm, ΔA_n is highest under saturated light, and decreases as light intensity decreases (Fig. 4a). ΔA_n is relatively constant and negative across all light intensities at 400 ppm CO_2 (Fig. 4c). The change of J_{max}/V_{cmax} also increases the ΔA_n and space for C_4 advantage under different light intensities (Fig. 4 b, d).

Finally, we calculate the photosynthesis rates of the two pathways under conditions often encountered in today's grasslands to look at the effect of nitrogen reallocation between RuBP carboxylation and regeneration: CO_2 =400 ppm, saturated light with three water conditions (Fig. 5). With J_{max}/V_{cmax} =2.1 for both C_3 and C_4, the C_4 assimilation rate is rarely higher than C_3, which indicates C_4 does not have an obvious advantage under current CO_2 from saturated water conditions through to VPD = 2 kPa and Ψ_S = -1 MPa in current grassland because of the cost of the CCM. However, with J_{max}/V_{cmax} =4.5 for C_4, C_4 does have an advantage over C_3 at temperatures above 25 ^oC.

Discussion

Changes in the climate that occurred towards the end of the Oligocene about 30 MYA led to a drier Earth; the consequent increase in wildfires and seasonal droughts forced the forests then covering the earth to give way to entirely new biomes: the grasslands and savannas (Strömberg 2011). The open and drier habitats populated by these ancestral grasses would have had higher temperatures due to greater incident radiation and an uncoupling from the turbulent mixing of air above the grass canopy, which exacerbate physiological challenges by increasing water loss from the leaf to the atmosphere. Furthermore, higher temperatures and a decrease in atmospheric CO_2 would have increased photorespiration in these ancestral C_3 grasses. Therefore, grasses encountered several environmental changes during the evolution of C_4: CO_2, temperature, water availability, increasing irradiance, and the reallocation of nutrients as the CCM evolved. Previous work has considered most of these factors separately, meaning potential interactions between them remain unexplored. We took a comprehensive approach to elucidate the multi-faceted selective pressures on early C_4 grassland evolution, the expansion of C_4 5-10 MYA and current distribution in an optimization framework.

Selective pressures and interactions among CO_2, temperature, water availability and light

We find that water limitation is the primary selective pressure for the evolution of C_4 grasses when CO_2 is above 400 ppm, suggesting that the environmental pressures for C_4 evolution were in place during the early expansion of grass-dominant biomes. During the early origins of C_4 (25-30 MYA), estimates of CO_2 concentrations are typically above 400 ppm (Cerling et al. 1997, Kürschner et al. 2008, Edwards & Smith 2010). Under saturated water conditions, the predicted crossover temperature at 400 ppm is above 40 °C because the benefits of the CCM are outweighed by the costs, indicating there is little room for C_4 to evolve. However, as water becomes more limited, the predicted crossover temperature ranges between 20 °C to 30 °C, while the C_4 advantage (ΔA_n) becomes increasingly larger due to the higher WUE conferred by the C_4 CCM. Our work therefore adds to the growing body of evidence that the primary selective factor for C_4 grass evolution was enhanced carbon gain under water limited conditions, in accordance with phylogenetic evidence (Edwards et al. 2010, Pau et al. 2013), and what has generally been believed to be the selective force behind the evolution of C_4 in dicotyledonous plants (Sage 2004).

In a recent physiological model, Osborne and Sack (2012) also suggest a hydrological underpinning to the competitive success of C_4 grasses, but found a much smaller environmental window for C_4 evolution than we did. At 400 ppm and Ψ_S = -1 MPa, they showed that C_4 hydraulic conductance must be twice that of C_3 grasses for C_4 grasses to achieve greater carbon uptake. In contrast, we find a clear C_4 advantage under these—

and even drier— conditions by allowing for optimal solutions of r_s and f to maximize A_n, while keeping plant hydraulic conductance equal across C_3 and C_4. Our results do not contradict the idea that larger bundle sheaths and smaller IVD— which were prerequisites for C_4 evolution (Griffiths et al. 2012, Christin et al. 2013) — led to greater hydraulic conductance among C_3 grass progenitors (Griffiths et al. 2012), but they do suggest that greater hydraulic conductance is not necessary to give C_4 plants an advantage once the CCM evolved.

As CO_2 decreased through the Miocene, C_4 grasses saw a large-scale global expansion 5-10 MYA. Our results suggest that at this time, the main selective force for C_4 evolution shifted from water limitation to low CO_2 and, to a lesser extent, light intensity. Low CO_2 provides a clear advantage for C_4 under all water availability and light intensity regimes. Under low CO_2, the greatest ΔA_n occurs in relatively saturated-water and mild-water-limited conditions, opposite what is seen under high CO_2, and suggesting water limitation is not as effective of a selective pressure under low CO_2. Our results are consistent with previous studies showing that low CO_2 (200-300 ppm) is a selective pressure for C_4 species (e.g. Ehleringer et al. 1997).

Since light intensity is not an important selective force under high CO_2, it seems likely that C_4 grasses could not dominate open grasslands, except in very arid areas, while CO_2 was still high. However, when CO_2 decreased to ~300 ppm and below (Cerling et al.

1997, Kürschner et al. 2008, Edwards & Smith 2010), high light intensity provided an enhanced advantage for C_4 (crossover temperature decreases, and ΔA_n increases). These findings give mechanistic support to the idea that between the initial evolutionary events leading to the emergence of C_4 grasses and the large-scale expansion 5-10 MYA, C_4 radiation idled in small pockets of selective favorability as CO_2 concentrations declined through the Miocene (Christin et al. 2008, Sage 2004). As CO_2 declined, the high light levels inherent to grassland systems gave C_4 photosynthesis an increasing selective advantage, leading to broader geographic and evolutionary radiation.

The role of nitrogen allocation in C_4 evolution and expansion

We assumed that during the early evolution of the CCM, both C_3 and C_4 plants had a similar balance of nitrogen across the light and dark reactions. Subsequent to the evolution of CCM, selection could favor the reallocation of nitrogen from dark to light reactions (increasing J_{max}/V_{cmax}). In general, CCMs allow for less investment in nitrogen-rich Rubisco (Ku et al. 1979, Christin & Osborne 2014), and the nitrogen not used for Rubisco could be either reinvested in light harvesting machinery, or simply not used at all. Increasing J_{max}/V_{cmax} almost always increases the photosynthesis rate of C_4 grasses (Fig. S2), and therefore could lead to a competitive advantage over C_3 grasses as well as C_4 grasses that do not reallocate. Assuming there is little cost or no genetic constraints for reallocation, the selection pressure to reallocate would have been strongest when CO_2 was high, i.e., during the initial evolutionary events in the

Oligocene/Miocene, when the CCM alone does not give C_4 a large advantage (low ΔA_n in Fig. 3c). When CO_2 was low during the C_4 radiation 5-10 MYA, however, the CCM alone would give C_4 an advantage and reallocation would not change the competitive balance between C_3 and C_4. As CO_2 remained low through to the Pleistocene, selection for nitrogen reallocation to the light reactions would lessen further, especially during the CO_2 minima of the Pleistocene glacial periods (~ 180 ppm). In this context, an interesting question is whether the high CO_2 of the last 150 years is selecting for increased J_{max}/V_{cmax} today.

Modeling studies have assumed a high J_{max}/V_{cmax} for C_4 photosynthesis, while the few empirical estimates of J_{max}/V_{cmax}, in C_4 plants paint a more variable picture for extant C_4 species. C_4 photosynthesis models assumed J_{max}/V_{cmax} to be around 4.5 with the same sum of J_{max} and V_{cmax} for C_3 and C_4 (Vico & Porporato 2008, using a fit from Collatz et al. 1992, Osborne & Sack 2012). C_4 species have lower Rubisco content and higher chlorophyll and thylakoid content, giving evidence of reallocation in extant C_4 species (Tissue et al. 1995, Ghannoum et al. 2010, Vogan & Sage 2012). In contrast, empirically-based estimates of C_4 J_{max}/V_{cmax} range from less than 2 to above 6, with a mean of about 4 (Domingues et al. 2007, Massad et al. 2007, Grant et al. 2007, Kathilankal et al. 2011, Ye et al. 2013, Ge et al. 2014), which is lower than model assumptions, but still higher than the mean J_{max}/V_{cmax} estimates for C_3 plants of 2.1 (Wullschleger 1993). Our results suggest that nitrogen availability and environmental factors (water, CO2, light) have likely affected natural variation in J_{max}/V_{cmax} observed in extant species, as well as through evolutionary time.

Conclusion

Our results show that by optimizing carbon gain over water loss, we can tease apart the selective factors for C_4 evolution in the grasses in both the relatively high CO_2 conditions of the late Oligocene/Early Miocene and the late Miocene expansion. At any CO_2 concentration above 400 ppm, water limitation was the primary selective factor for C_4 evolution, and even at 600 ppm there is room for C_4 evolution under the driest conditions. Furthermore, we find that the CCM alone leads to enough of a reduction in water use that there would have been little selection for increased hydraulic conductance within C_4 grasses. Below 400 ppm, CO_2 and to a lesser extent light, become the dominant selective pressures, leading to gains in net C_4 carbon assimilation that greatly exceeded those under higher CO_2. We therefore have a plausible physiological explanation for why C_4 grasses could have evolved hand-in-hand with the grassland biome, even though they did not achieve ecological dominance for many millions of years until CO_2 concentrations dropped.

C_4 photosynthesis first evolved in the grasses 25 – 32 MYA, and many subsequent and independent evolutionary origins occurred well into the Pleistocene 2.8 MYA. Each evolutionary origin potentially represents both different selective pressures and taxonomic (genetic) constraints as climate and CO_2 changed. Taking the Chloridoideae as an example, our model suggests that initial evolution of C_4 photosynthesis 25 – 32 MYA (Christin et al. 2008) was driven by aridity, acting to decrease stomatal conductance that increased photorespiration in C_3 progenitors initially, and led to higher water use efficiency upon the evolution of the CCM. Also at this point, there would have been strong selection for reallocation of nitrogen from the dark reactions to the light reactions. The large radiation of C_4 within the Chloridoideae that occurred 5 – 10 MYA was likely driven by low CO_2 and high light. There would have been much less selective pressure to reallocate N at this point, but such a reorganization was likely already in place within the clade. In contrast, for the lineages that first evolved C_4 in the late Miocene (e.g. *Stipagrostis*, *Eriachne*, *Neurachne*), CO_2 would have been the primary impetus for C_4 evolution, but for these lineages there would have been little impetus to reallocate nitrogen until the dawn of the industrial revolution. In many ways this examination of nitrogen allocation is speculative, but it nonetheless illustrates how we can use comprehensive physiological models to tease apart variation in C_4 physiology along the evolutionary trajectory. Furthermore, by selecting extant species within select lineages, nitrogen stoichiometry can be examined empirically, ultimately providing an integrative view of the selection pressures that led to the extant physiology and distribution of C_4 plants.

Acknowledgements

We are grateful for support from the University of Pennsylvania as well as undying assistance from Qing Zhang, Jemma Lloyd-Helliker and Ebru Erdem-Akçay.

References

1. von Caemmerer, S. (2000). Biochemical models of photosynthesis. In Techniques in Plant Sciences. CSIRO Publishing, Colingwood, Australia, pp 91–122.

2. Cerling, T.E., Harris, J.M., MacFadden, B.J., Leakey, M.G., Quade, J., Eisenmann, V. & Ehleringer, J.R. (1997). Global vegetation change through the Miocene/Pliocene boundary. Nature, 389, 153-158.

3. Chen, D.-X., Coughenour, M.B., Knapp, A.K. & Owensby, C.E. (1994). Mathematical simulation of C_4 grass photosynthesis in ambient and elevated CO_2. Ecol. Model., 73, 63–80.

4. Christin P.A., Besnard G., Samaritani E., Duvall M.R., Hodkinson T.R., Savolainen V. & Salamin N. (2008). Oligocene CO2 decline promoted C_4 photosynthesis in grasses. Curr. Biol., 18, 37–43.

5. Christin, P.A., Osborne, C.P., Chatelet, D.S., Columbus, J.T., Besnard, G., Hodkinson, T.R., Garrison, L.M., Vorontsova, M.S. & Edwards, E.J. (2013). Anatomical enablers and the evolution of C_4 photosynthesis in grasses. Proc. Natl. Acad. Sci. USA, 110, 1381-1386.

6. Christin, P.A. & Osborne, C.P. (2014). Tansley Review. The evolutionary ecology of C_4 photosynthesis. New Phytol., 204, 765-781.

7. Collatz, G.J., Berry, J.A. & Clark, J.S. (1998). Effects of climate and atmospheric CO_2 partial pressure on the global distribution of C_4 grasses: present, past, and future. Oecologia, 114, 441-454.

8. Collatz, G.J., Ball, J.T., Grivet, C. &Berry, J.A. (1992). Coupled photosynthesis-stomatal conductance model for leaves of C_4 plants. Aust. J. Plant Physiol., 19, 519-538.

9. Domingues, T.F., Martinelli, L.A. & Ehleringer, J.R. (2007). Ecophysiological traits of plant functional groups in forest and pasture ecosystems from eastern Amazônia, Brazil. Plant Ecol., 193, 101-112.

10. Edwards, E.J., Osborne, C.P., Strömberg, C.A.E., Smith, S.A. & C4 Grasses Consortium. (2010). The Origins of C_4 Grasslands: Integrating Evolutionary and Ecosystem Science. Science, 328, 587-591.

11. Edwards, E.J. & Smith, S.A. (2010). Phylogenetic analyses reveal the shady history of C_4 grasses. Proc. Natl. Acad. Sci. USA, 107, 2532-2537.

12. Edwards, E.J. & Still, C.J. (2008). Climate, phylogeny and the ecological distribution of C_4 grasses. Ecol. Lett., 11, 266-276.

13. Ehleringer, J.R. & Monson, R.K. (1993). Evolutionary and ecological aspects of photosynthesis pathway variation. Annu. Rev. Ecol. Syst., 24, 411-439.

14. Ehleringer, J.R., Cerling, T.E. & Helliker, B.R. (1997). C_4 photosynthesis, atomospheric CO_2, and climate. Oecologia, 112, 285-299.

15. Farquhar, G.D., Von Caemmerer, S. & Berry, J.A. (1980). A biochemical model of photosynthetic carbon dioxide assimilation in leaves of 3-carbon pathway species. Planta, 149, 78–90.

16. Ge, Z.M., Zhang, L.Q., Yuan, L. & Zhang, C. (2014). Effects of salinity on temperature-dependent photosynthetic parameters of a native C3 and a non-native C4 marsh grass in the Yangtze Estuary, China. Photosynthetica, 52, 484–492.

17. Ghannoum, O. (2009). C_4 photosynthesis and water stress. Ann. Bot., 103, 635–644.

18. Ghannoum, O., Evans, J.R. & von Caemmerer, S. (2010). Nitrogen and water use efficiency of C_4 plants. In: *C_4 photosynthesis and related CO_2 concentrating mechanisms* (eds. Raghavendra, A.S. & Sage, R.F.). Springer Science, The Netherlands, Dordrecht, pp. 129–146.

19. Givnish, T.J. (1986). Optimal stomatal conductance, allocation of energy between leaves and roots, and the marginal cost of transpiration. In: *On the Economy of Plant Form and Function* (ed. Givnish TJ). Cambridge University Press, Cambridge, pp. 171–213.

20. Grant, R.F. & Flanagan, L.B. (2007). Modeling stomatal and nonstomatal effects of water deficits on CO_2 fixation in a semiarid grassland. J. Geophys. Res.,112, G03011, doi:10.1029/2006JG000302.

21. Griffiths, H., Weller, G., Toy, L. & Dennis, R.J. (2012). You’re so vein: bundle sheath physiology, phylogeny and evolution in C_3 and C_4 plants. Plant Cell Environ., 36, 249–261.

22. Hatch, M.D. (1987). C_4 photosynthesis: a unique blend of modified biochemistry, anatomy and ultrastructure. Biochim. Biophys. Acta, 895, 81-106.

23. Kathilankal, J.C., Mozdzer, T.J., Fuentes, J.D., McGlathery, K.J., D'Odorico, P. & Zieman, J.C. (2011). Physiological responses of Spartina alterniflora to varying environmental conditions in Virginia marshes. Hydrobiologia, 669, 167-181.

24. Ku, M.S.B., Schmitt, M.R. & Edwards, G.E. (1979). Quantitative determination of RuBP carboxylase-orygenase protein in leaves of several C_3 and C_4 plants. J. Exp. Bot., 114, 89–98.

25. Kürschner, W.M., Kvacek, Z. & Dilcher, D.L. (2008). The impact of Miocene atmospheric carbon dioxide fluctuations on climate and the evolution of terrestrial ecosystems. Proc. Natl. Acad. Sci. U S A, 105, 449-453.

26. Lawlor, D.W. & Cornic, G. (2002). Photosynthetic carbon assimilation and associated metabolism in relation to water deficits in higher plants. Plant Cell Environ., 25, 275–294.

27. Massad, R.S., Tuzet, A. & Bethenod, O. (2007). The effect of temperature on C_4-type leaf photosynthesis parameters. Plant Cell Environ., 30, 1191-1204.

28. Medlyn, B.E., Duursma, R.A., Eamus, D., Ellsworth, D.S., Prentice, I.C., Barton, C.V.M., Crous, K.Y., De Angelis, P., Freeman, M. & Wingate, L. (2011). Reconciling the optimal and empirical approaches to modelling stomatal conductance. Glob. Chang Biol., 17, 2134-2144.

29. Osborne, C. P. (2008). Atmosphere, ecology and evolution: what drove the Miocene expansion of C_4 grasslands? J. Ecol., 96, 35-45.

30. Osborne, C.P. & Freckleton, R.P. (2009). Ecological selection pressures for C_4 photosynthesis in the grasses. Proc. Biol. Sci., 276, 1753-1760.

31. Osborne, C.P. & Sack, L. (2012). Evolution of C_4 plants: a new hypothesis for an interaction of CO_2 and water relations mediated by plant hydraulics. Philos. Trans. R. Soc. Lond. B. Biol. Sci., 367, 583-600.

32. Pau, S., Edwards, E.J. & Still, C.J. (2013). Improving our understanding of environmental controls on the distribution of C_3 and C_4 grasses. Glob. Chang Biol., 19, 184-196.

33. Prentice, I. C., Dong, N., Gleason, S.M., Maire, V. & Wright, I.J. (2014). Balancing the costs of carbon gain and water transport: testing a new theoretical framework for plant functional ecology. Ecol. Lett. 17, 82-91.

34. Sage, R.F. (2004). The evolution of C4 photosynthesis. New Phytol., 161, 341-370.

35. Sage, R.F., Sage, T.L. & Kocacinar F. (2012). Photorespiration and the evolution of C_4 photosynthesis. Annu. Rev. Plant Biol., 63, 19-47.

36. Strömberg, C.A.E. (2011). Evolution of grasses and grassland system. Annu. Rev. Earth Planet Sci., 39, 517-544.

37. Tang, A.C. (2002). Photosynthetic oxygen evolution at low water potential in leaf discs lacking an epidermis. Ann. of Bot., 89, 861-870.

38. Taylor, S.H., Franks, P.J., Hulme, S.P., Spriggs, E., Christin, P.A., Edwards, E.J., Woodward, F.I. & Osborne, C.P. (2012). Photosynthetic pathway and ecological adaptation explain stomatal trait diversity amongst grasses. New Phytol., 193, 387-396.

39. Taylor, S.H., Ripley, B.S., Martin, T., De-Wet, L.-A., Woodward, F.I. & Osborne, C.P. (2014). Physiological advantages of C_4 grasses in the field: a comparative experiment demonstrating the importance of drought. Glob. Change Biol., 20, 1922-2003.

40. Tezara, W., Mitchell, V.J., Driscoll, S.D. & Lawlor, D.W. (1999). Water stress inhibits plant photosynthesis by decreasing coupling factor and ATP. Nature, 401, 914-917.

41. Tissue, D.T., Griffin., K.L., Thomas, R.B. & Strain, B.R. (1995). Effects of low and elevated CO_2 on C_3 and C_4 annuals. II. Photosynthesis and leaf biochemistry. Oecologia, 101, 21-28.

42. Vico, G. & Porporato, A. (2008). Modelling C_3 and C_4 photosynthesis under water-stressed conditions. Plant and Soil, 313, 187-203.

43. Vogan, P.J. & Sage R.F. (2012). Effects of low atmospheric CO_2 and elevated temperature during growth on the gas exchange responses of C_3, C_3–C_4 intermediate,

and C_4 species from three evolutionary lineages of C_4 photosynthesis. Oecologia, 169, 341-352.

44. Way, D.A., Katul, G.G., Manzoni, S. & Vico, G. (2014). Increasing water use efficiency along the C_3 to C_4 evolutionary pathway: a stomatal optimization perspective. J. Exp. Bot., 65, 3683-3693.

45. Wullschleger, S.D. (1993). Biochemical limitations to carbon assimilation in C_3 plants - A retrospective analysis of the A/C_i curves from 109 species. J. Exp. Bot., 44, 907-920.

46. Ye Z., Suggett, D.J., Robakowski, P., Kang, H. (2013). A mechanistic model for the photosynthesis-light response based on the photosynthetic electron transport of photosystem II in C_3 and C_4 species. New Phytol., 199: 110–120.

Figure Legends

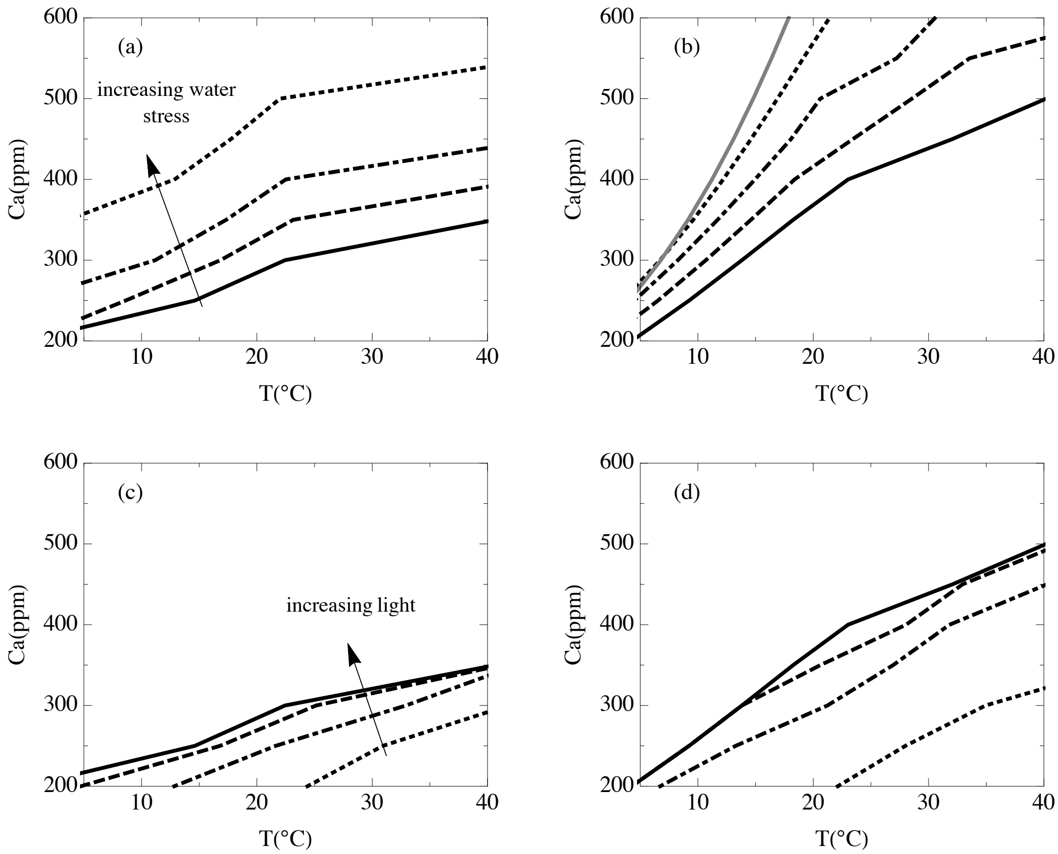

Fig. 1. (a) Crossover temperatures of photosynthesis for C_3 and C_4 with the change of CO_2 concentration under different water conditions. Light intensity was 1400 μmol photons $m^{-2}s^{-1}$ and J_{max}/V_{cmax}=2.1 for C_3 and C_4; (b) same as (a) except J_{max}/V_{cmax}=2.1 for C_3 and J_{max}/V_{cmax}=4.5 for C_4. Solid black line: VPD=0.15kPa, Ψ_S=0 MPa; dashed black line: VPD=1kPa, Ψ_S=-0.5 MPa; dot-dashed black line: VPD=2kPa, Ψ_S=-1 MPa; dotted black line: VPD=3 kPa, Ψ_S=-1.5 MPa; solid gray line: VPD=4 kPa, Ψ_S=-2 MPa. (c) Crossover temperatures with the change of CO_2 concentration under different light intensities under saturated water condition (VPD=0.15kPa, Ψ_S=0 MPa). J_{max}/V_{cmax}=2.1 for C_3 and C_4, (d) same as (c) except J_{max}/V_{cmax}=2.1 for C_3 and J_{max}/V_{cmax}=4.5 for C_4.

Solid black line: 1400 µmol photons $m^{-2}s^{-1}$; dashed black line: 1000 µmol photons $m^{-2}s^{-1}$; dot-dashed black line: 600 µmol photons $m^{-2}s^{-1}$; dotted black line: 200 µmol photons $m^{-2}s^{-1}$.

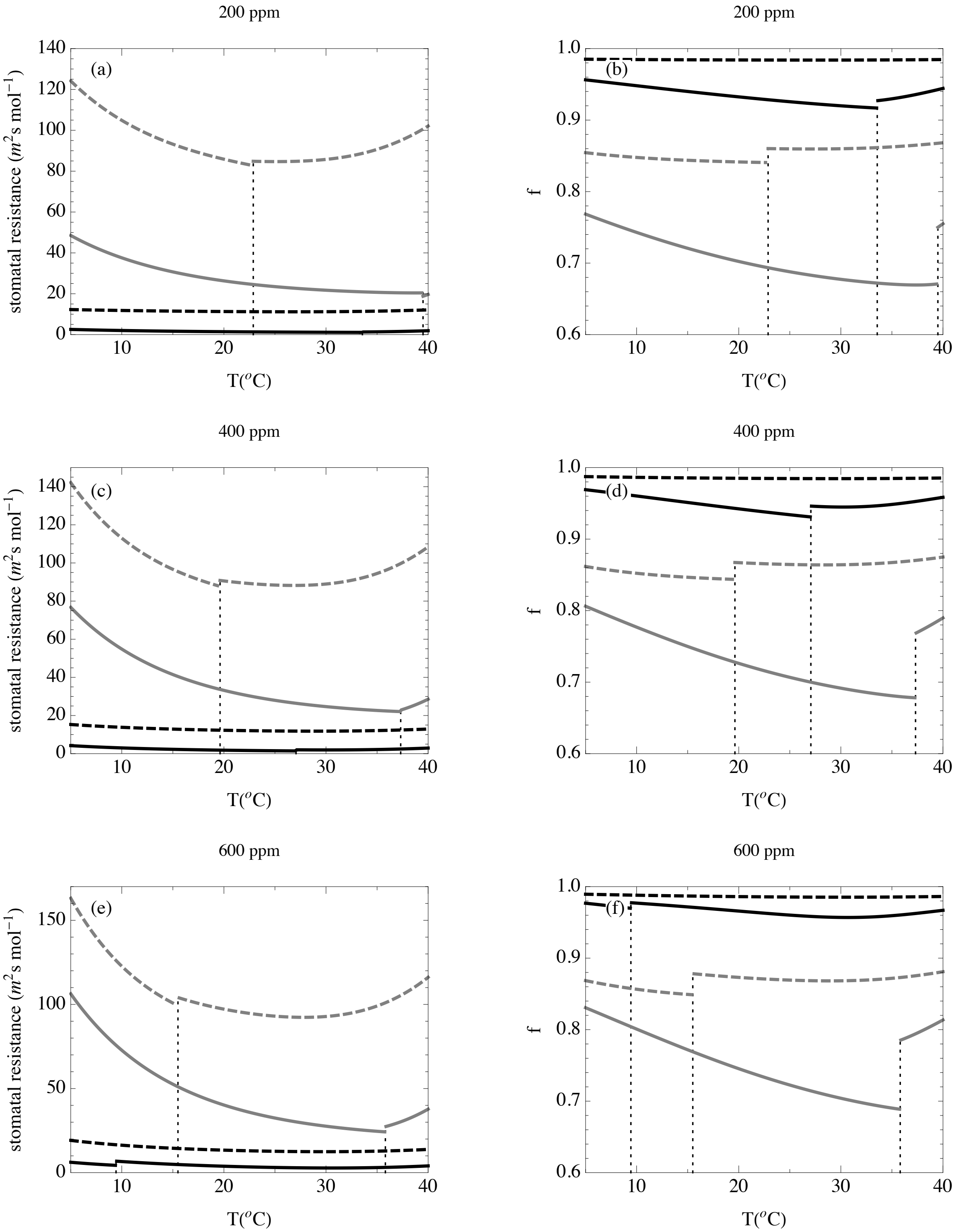

Fig. 2. Stomatal resistance (r_s) and leaf allocation (f) as a function of temperature, with J_{max}/V_{cmax}=2.1 for both C_3 and C_4 with saturated light under different CO_2 (200 ppm, 400

ppm and 600 ppm) and different water conditions. Solid black line: C_3 with VPD=0.15kPa, Ψ_S=0 MPa; dashed black line: C_4 with VPD=0.15kPa, Ψ_S=0; solid grey line: C_3 with VPD=4 kPa, Ψ_S=-2 MPa; dashed grey line: C_4 with VPD=4 kPa, Ψ_S=-2 MPa. Vertical lines indicate transition from RuBP carboxylation limited condition to RuBP regeneration limited condition for C_3; for C_4, all the transition temperatures<5 °C.

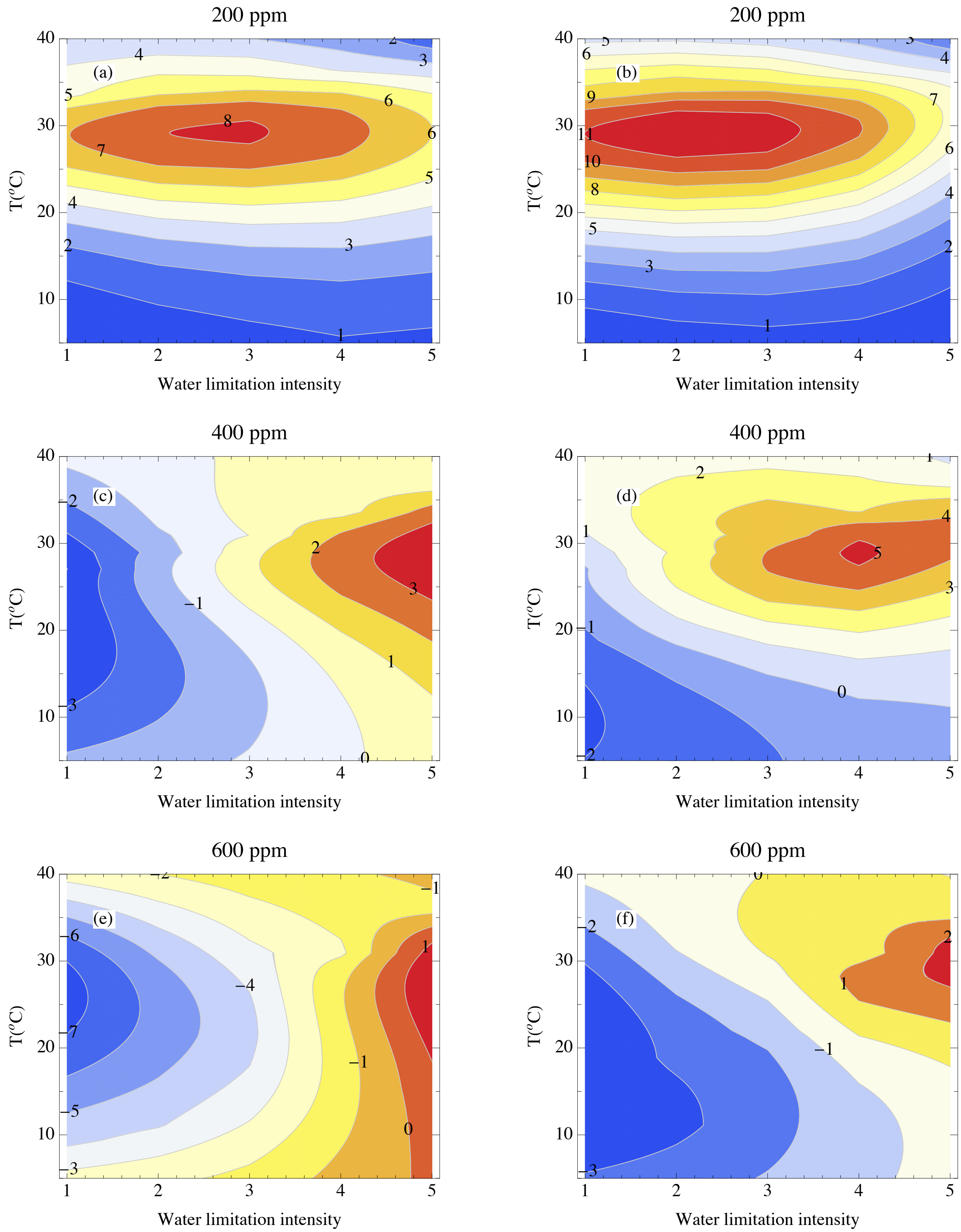

Fig. 3. Contour plot of modeled assimilation difference between C_4 and C_3 ($A_n(C_4)$-$A_n(C_3)$) with J_{max}/V_{cmax}=2.1 for C_3 and C_4 under various CO_2 (200 ppm, 400 ppm

and 600 ppm) and saturated light intensity (1400 µmol photons $m^{-2}s^{-1}$), various water conditions (a, c, e) and with J_{max}/V_{cmax}=2.1 for C_3 and J_{max}/V_{cmax}=4.5 for C_4 (b, d, f). Water limitation intensity 1, 2, 3, 4, 5 refers to VPD=0.15kPa, Ψ_S=0 MPa; 1.5 kPa, -0.5MPa; 2kPa, -1 MPa; 3kPa, -1.5 MPa; 4kPa, -2 MPa.

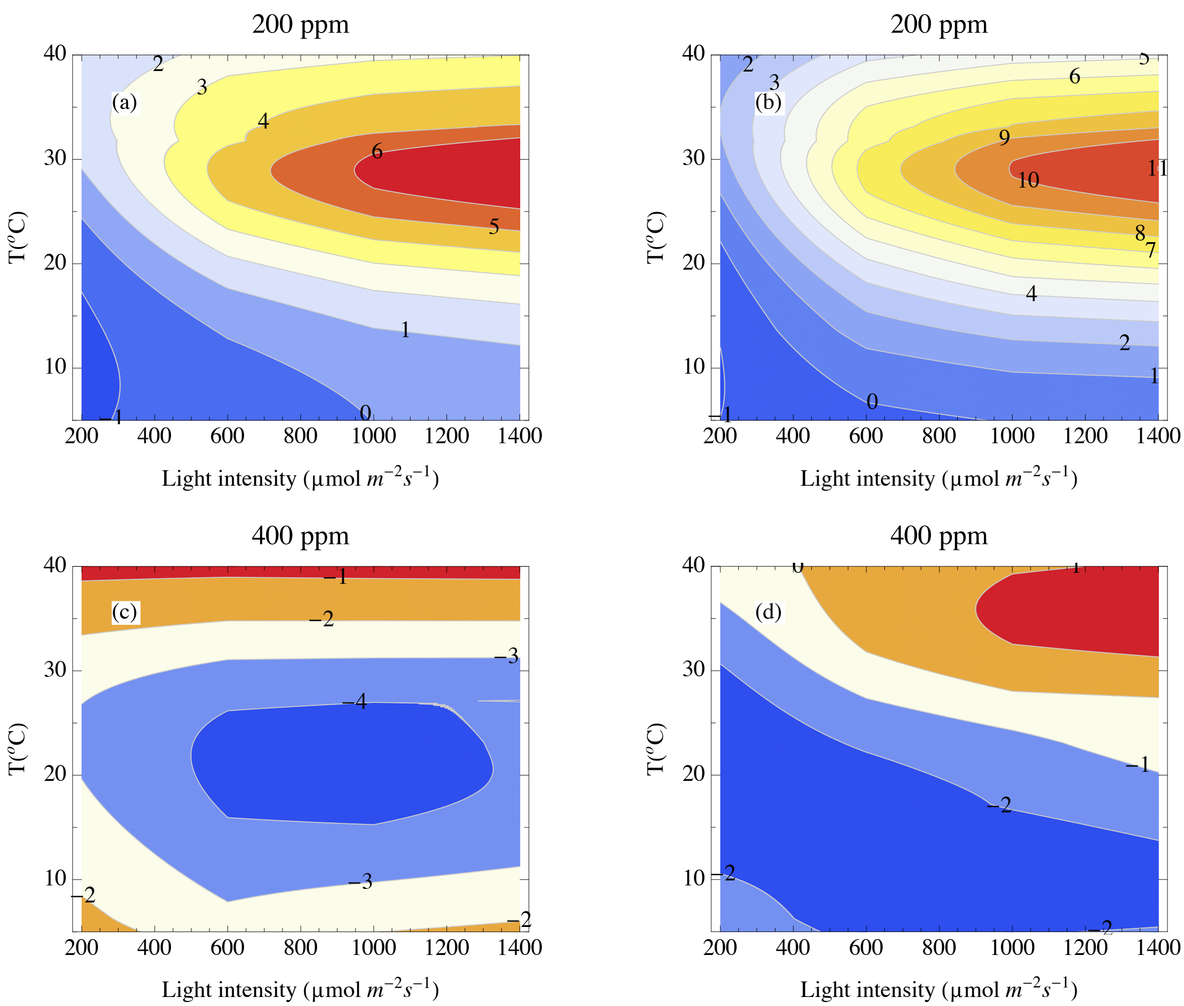

Fig. 4. Contour plot of modeled assimilation difference between C_4 and C_3 ($A_n(C_4)$-$A_n(C_3)$) with J_{max}/V_{cmax}=2.1 for C_3 and C_4 under various CO_2 (200 ppm, 400 ppm) and different light intensities (from 200 to 1400 µmol photons $m^{-2}s^{-1}$) with saturated water

condition (VPD=0.15kPa, Ψ_S=0 MPa) (a, c) and with J_{max}/V_{cmax}=2.1 for C_3 and J_{max}/V_{cmax}=4.5 for C_4 (b, d).

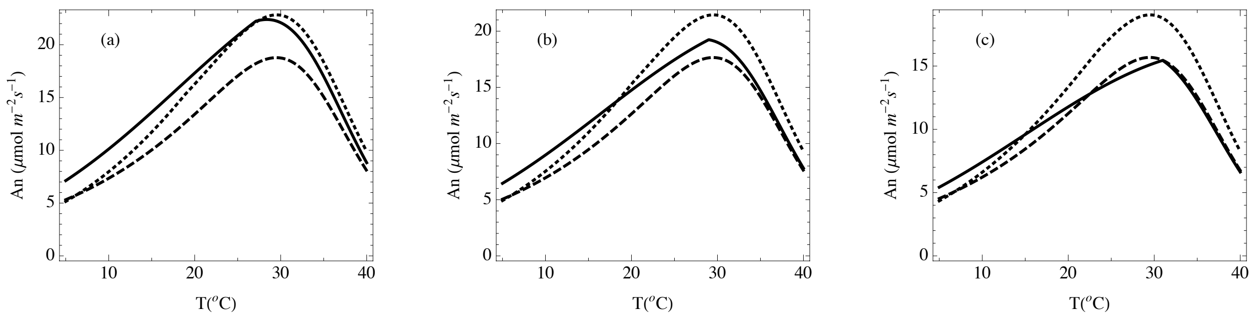

Fig. 5. Assimilation rates of C_3 with J_{max}/V_{cmax}=2.1 (solid black line), C4 with J_{max}/V_{cmax}=2.1 (dashed black line) and C_4 with J_{max}/V_{cmax}=4.5 (dotted black line) under light intensity of 1400 µmol photons $m^{-2}s^{-1}$, CO_2 of 400 ppm and different water limitated conditions. (a) saturated soils; (b) VPD=1kPa and Ψ_S=-0.5 MPa; (c) VPD=2kPa and Ψ_S=-1 MPa.